

Aperiodic multilayer graphene based tunable and switchable thermal emitter at mid-infrared frequencies

S. Sharifi, Y. M. Banadaki, V. F. Nezhad, G. Veronis, and J. P. Dowling

Citation: *Journal of Applied Physics* **124**, 233101 (2018); doi: 10.1063/1.5048332

View online: <https://doi.org/10.1063/1.5048332>

View Table of Contents: <http://aip.scitation.org/toc/jap/124/23>

Published by the *American Institute of Physics*

Ultra High Performance SDD Detectors



See all our XRF Solutions

Aperiodic multilayer graphene based tunable and switchable thermal emitter at mid-infrared frequencies

S. Sharifi,^{1,2,3,a)} Y. M. Banadaki,^{3,4} V. F. Nezhad,^{1,2} G. Veronis,^{1,2} and J. P. Dowling^{3,5,6,7}

¹Center for Computation and Technology, Louisiana State University, Baton Rouge, Louisiana 70808, USA

²School of Electrical Engineering & Computer Science, Louisiana State University, Baton Rouge, Louisiana 70803, USA

³Hearne Institute for Theoretical Physics, Department of Physics and Astronomy, Louisiana State University, Baton Rouge, Louisiana 70803, USA

⁴School of Computer Science, Southern University and A&M College, Baton Rouge, Louisiana 70813, USA

⁵NYU-ECNU Institute of Physics at NYU Shanghai, Shanghai 200062, China

⁶CAS-Alibaba Quantum Computing Laboratory, USTC, Shanghai 201315, China

⁷National Institute of Information and Communications Technology, Tokyo 184-8795, Japan

(Received 13 July 2018; accepted 2 December 2018; published online 17 December 2018)

Graphene attracts enormous interest for photonic applications as it provides a degree of freedom to manipulate electromagnetic waves. In this paper, we present new graphene-based aperiodic multilayer structures as selective, tunable, and switchable thermal emitters at infrared frequencies. For these optimized aperiodic thermal emitters, we investigate the effect of the chemical potential and number of graphene layers on the range of selectivity, tunability, and switchability of thermal emittance. We find that the proposed thermal emitters show about an order of magnitude narrower thermal band, e.g., improved selectivity. The tunability of thermal power emitted from the structure with 32 graphene layers is ~ 3.5 times larger than that of the structure with eight graphene layers, changing from $\lambda = 3.34 \mu\text{m}$ to $2.85 \mu\text{m}$ by increasing the chemical potential from 0.0 eV to 1.0 eV. We demonstrate that the arrangement with 32 graphene layers can decrease by $\sim 83\%$ of the power emitted for $\lambda = 3.34 \mu\text{m}$, providing ~ 4.5 times stronger switchability than for the structure with eight graphene layers. The electrically dynamic control of the proposed graphene-based aperiodic multilayer structures can pave the way for a new class of *in situ* wavelength selective, tunable, and switchable thermal sources. *Published by AIP Publishing.* <https://doi.org/10.1063/1.5048332>

I. INTRODUCTION

At finite temperatures, all materials emit electromagnetic radiation due to the thermally induced motion of particles and quasiparticles.¹ A perfect thermal emitter follows Planck's law of blackbody radiation, which is broadband, incoherent, and isotropic, with a spectral profile and intensity that are dependent on the emissivity of a material and vary only with changes in temperature. The spectral features of the thermal emission (e.g., wavelength, bandwidth, peak emissivity, and angular characteristics) are strongly dependent on the choice of both materials and structures of the emitters. However, it is desirable to realize an arbitrary shaping of thermal emission spectra that radiates only within a specific frequency bandwidth, e.g., a single-peak ultranarrowband emission for mid-infrared (IR) sensing² or a stepwise emissivity spectrum for thermophotovoltaics.³ Coherent infrared thermal radiation with tunable emitting frequencies in a broad spectral range is highly desired for numerous promising applications in energy harvesting,⁴ chemical sensing,⁵ infrared (IR) sources,⁶ thermal circuits,⁷ antennae,⁸ and radiative cooling.⁹ Nanoengineered structures can control the directionality and coherence of blackbody emission as patterned gratings,^{10,11} photonic crystals,^{12,13} microcavity resonators,^{14,15} metasurfaces,^{1,16} and graphene

nanostructures.¹⁷ Photonic bandgaps can achieve a selective emitter in photonic crystals composed of metallic and dielectric structures.^{10,18} Electromagnetic fields are strongly decreased below the plasma frequency of metals,^{19,20} and thereby they introduce flexibility in creating a thermal emitter with broadband frequency selectivity.^{21,22} Also, metals are potentially suitable for near-infrared selective thermal emitters, since they have significant absorption in these frequencies with stable properties at high temperatures. However, conventional metals have high reflectivity in mid- and far-infrared frequencies and consequently structures composed of metals can potentially exhibit low emissivity.²³ As such, the surface is required to be modified periodically by an array of grooves²⁴ or holes²² to enhance emission at infrared frequencies.

A narrowband thermal emission can be achieved using metallic nanostructures so that the optical resonant modes, confined in the so-called Fabry–Perot cavity,²⁵ are excited on the metal surface, leading to enhanced emissivity at those resonant wavelengths.^{16,26} According to the Purcell effect,²⁷ thermal radiation from an optical resonator can be dramatically modulated by the resonance mode designed in the infrared range, leading to narrow-band thermal emission at the resonant frequency. Liu *et al.*²⁸ demonstrated that the matched mode of the emitter could be lost when the resonance mode is electrically quasi-static, i.e., the electric field oscillates in phase, resulting in the fundamental limit of the

^{a)}Author to whom correspondence should be addressed: sshari2@lsu.edu

spectral thermal emission power from an optical resonator. Metamaterials based structures have also led to narrowband thermal emission.^{29,30} The effective permittivity and permeability of the entire formation are artificially controlled by combining subwavelength metallic elements with thin dielectric layers in a properly designed structure, leading to perfect emittance (maximum emission) at the resonant wavelengths.³¹ However, the strong free carrier absorption due to metals leads to undesired radiation over an extensive wavelength range together with the broadening of the emission peaks in selective thermal emitters designed by photonic crystals and metamaterials.³² Moreover, a narrowband resonance achieved in these structures cannot be changed dynamically to other operating frequencies due to the limitation in the properties and functionalities of available conventional metals.

The dynamic control of thermal radiation has been demonstrated through *in situ* modification of material emissivity. This control has been achieved with nanophotonic structures that incorporate phase change materials so that the emissivity can be electronically manipulated by controlling the charge injection and consequently the polariton modes in the structure. Cong *et al.*³³ demonstrated that a tunable selective absorber could be designed by InSb, whose carrier density can be adjusted by utilizing an optical pump or changing the surrounding temperature, altering the resonance frequency of split rings. Similarly, tunable perfect thermal emitters could be designed by the genesis of new materials.

Graphene, an atomic layer of carbon, has zero bandgap with high carrier mobility that allows strong interaction with terahertz and mid-infrared waves.³⁴ The propagation of these waves can be actively controlled by varying the chemical potential in graphene, which can be tuned by chemical doping, voltage bias, external magnetic field, or optical excitation.³⁵ As such, graphene provides a unique platform for electrically controlling the spectral properties of thermal emittance. The absorption coefficient of graphene exceeds $5 \times 10^7 \text{ m}^{-1}$ in the visible wavelength if it is normalized to its atomic thickness, which is more than ten times larger than those in gallium arsenide and silicon.³⁶ However, single-atom-layer of graphene has low single-pass optical absorption so that total absorption can be only achieved by novel designs of graphene-based nanostructures. Thongrattanasiri *et al.*¹⁷ demonstrated perfect tunable absorbers with graphene ribbon array on a dielectric spacer and a metallic substrate.^{17,36} Wang *et al.*³⁷ showed an infrared (IR) frequency-tunable selective thermal emitter made of graphene-covered silicon carbide (SiC) grating whose resonance frequency can be dynamically tuned by $\sim 8.5\%$ by varying graphene's chemical potential. Fang *et al.*³⁸ demonstrated tunable selective absorption in graphene disk arrays.

In this paper, we propose new graphene-based aperiodic multilayer structures as selective, tunable, and switchable infrared thermal emitters. We optimize the structures using the genetic optimization algorithm for the sake of narrowband thermal power at $\lambda = 3.34 \mu\text{m}$ for zero bias condition. For the optimized structures, we investigate the selectivity, tunability, and switchability of thermal emittance by varying the chemical potential of graphene layers. We demonstrate

that the *in situ* control over the chemical potential of graphene layers that can be electrically changed by the perpendicular electric field results in tunability of $0.5 \mu\text{m}$ at mid-infrared wavelengths for the structure with 32 graphene layers. We find that the emitted power of this structure significantly decreases at the optimized wavelength, introducing a promising design for dynamic switchability of thermal energy. We also investigate the effect of the number of graphene layers on the selectivity, tunability, and switchability of thermal emittance. Our results show that the structure with a more significant number of graphene layers has lower selectivity, but higher tunability and switchability.

The paper is organized as follows: Sec. II explains the structure of the proposed thermal emitters and provides the required theoretical background such as the optimization method and the optical conductivity of graphene. This section is followed by a discussion of the effect of changing the chemical potential on graphene's refractive index for designing a new class of tunable and switchable thermal sources. Then, in Sec. III, we demonstrate the optimized aperiodic multilayer structures composed of graphene and hexagonal Boron Nitride (hBN) layers. More specifically, we maximize the normalized power emitted from different aperiodic thermal emitters with 8, 13, 23, 28, and 32 sheets of graphene to the perfect value of unity for normal light incidence at a single mid-infrared wavelength. The rest of this section is dedicated to the simulation results including the effect of varying chemical potential of graphene and the number of graphene layers on the selectivity, tunability, and switchability of the proposed infrared thermal emitters. Finally, our conclusions are summarized in Sec. VI.

II. THEORY

The thermal radiation from bulk materials, e.g., tungsten, is characterized by incoherent, isotropic, and broadband radiation spectra, which is not a characteristic of the materials in the object and exclusively depends on the surface temperature of the object. An idealized blackbody absorbs all radiation that falls into the full range enforced by the temperature of the object. The thermal radiation spectra can be drastically altered by utilizing textured surfaces or aperiodic multilayer structures. The normalized power radiated per unit area and unit wavelength by a non-blackbody in the normal direction as a function of wavelength and temperature can be calculated as follows:

$$\bar{\mu}(\lambda) = \frac{\epsilon_{Total}(\lambda, T) B(\lambda, T)}{\max_{\lambda} [B(\lambda, T)]}, \quad (1)$$

where $B(\lambda, T)$ is the power radiated per unit area and unit wavelength, T is the ambient temperature, and λ is the wavelength. $\epsilon_{Total}(\lambda) = [\epsilon_{TE}(\lambda) + \epsilon_{TM}(\lambda)]/2$ is the averaged emittance of the optimized structures from both TE and TM polarizations in the normal direction. The value of $\bar{\mu}(\lambda)$ indicates how well the multilayer structure emits photons at a given wavelength in the normal direction. Figure 1 shows the schematic of our proposed structures composed of alternating layers of graphene and hBN insulator, which are sandwiched between two thick silicon carbide (SiC) layers. This

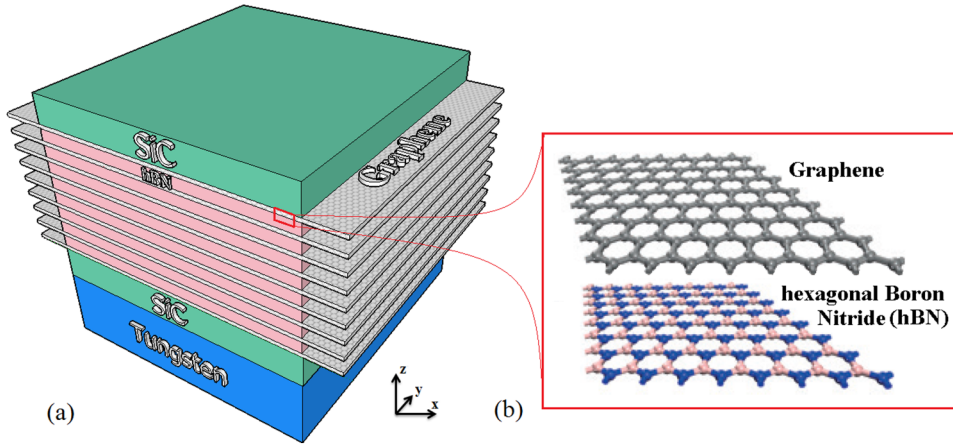


FIG. 1. (a) Structure of the proposed thermal emitter composed of alternating layers of graphene and hBN insulator, which are sandwiched between two thick silicon carbide (SiC) layers. A semi-infinite tungsten (W) layer is used as the substrate. (b) Lattice structures of graphene and hBN buffer monolayer have similar hexagonal honey-comb architectures.

aperiodic multilayer structure may provide spectra-altering properties similar to that of more complex and harder-to-fabricate two- or three-dimensional structures, indicating a proof of concept to design and implement more complex structures. The atomic thickness of hBN monolayers is ~ 0.33 nm, similar to graphene^{39,40} [Fig. 1(b)]. The hBN and graphene layers can be deposited layer-by-layer to construct a graphene-hBN heterostructure,⁴¹ providing accurate control of the spacing between the graphene layers in the proposed aperiodic multilayer structures. A semi-infinite tungsten (W) layer is used as the substrate. Since tungsten substrate is taken to be semi-infinite, the transmittance is identically zero, so that $A_{TE/TM}(\lambda) = 1 - R_{TE/TM}(\lambda)$, where $A_{TE/TM}(\lambda)$ is the TE/TM absorptance, $R_{TE/TM}(\lambda)$ is the TE/TM reflectance, and λ is the wavelength. The calculated absorptance can be equated to emittance ϵ_{Total} because of Kirchhoff's second law and conservation of energy under thermal equilibrium. Utilizing the transfer matrix method,¹² the absorptance, which is equal to the emittance, of the graphene-based structure is calculated.

We found that for a non-optimized multilayer structure with equally spaced graphene layers, not only the peak emittance is not close to the perfect value of unity but also the structure is not tunable. Thus, applying the genetic optimization algorithm is crucial to obtain a tunable and switchable thermal emitter. To find the optimum thicknesses of the

layers in the aperiodic multilayer structures, a hybrid optimization method⁴² consisting of a micro-genetic global optimization algorithm coupled to a local optimization algorithm is employed. The genetic algorithm is an iterative optimization procedure which starts with a randomly selected population of potential solutions and evolves toward improved solutions; once the population converges, the local optimization algorithm finds the local optimum. The process retains the best structure found and is iteratively repeated. Using this algorithm, the optimized thicknesses for maximizing the absorption coefficient to the perfect value of unity can be found at a prespecified wavelength and zero bias condition.⁴²

In the proposed structure, the density of charge carriers associated with the chemical potential in graphene layers can be controlled by applying a DC bias electric field perpendicular to the graphene/hBN surfaces, leading to the electrical control of graphene's refractive index.³⁵ However, the refractive index is not well defined for 2D graphene because there is no rigorous definition for the induced polarization per unit volume. A more suitable physical quantity to explain the optical properties of graphene is optical conductivity, a complex number associated with the surface current induced in graphene by light,⁴³ which is sensitively dependent on the chemical potential (Fermi energy). Graphene's conductivity may be modeled using the Kubo formula⁴⁴

$$\sigma_d(\omega, \mu_c, \Gamma, T) = -\frac{ie^2(\omega + i2\Gamma)}{\pi\hbar^2} \left[\frac{1}{(\omega + 2i\Gamma)^2} \int_0^\infty \left(\frac{\partial n_F(\epsilon)}{\partial \epsilon} - \frac{\partial n_F(-\epsilon)}{\partial \epsilon} \right) \epsilon d\epsilon - \int_0^\infty \frac{n_F(-\epsilon) - n_F(\epsilon)}{(\omega + 2i\Gamma)^2 - 4(\epsilon/\hbar)^2} d\epsilon \right], \quad (2)$$

where $n_F(\epsilon) = 1/\{1 + \exp[(\epsilon - \mu_c)/(k_B T)]\}$ is the Fermi-Dirac distribution, ω is the radian frequency, e is the electron charge, \hbar is the reduced Planck constant, T is the temperature, μ_c is the chemical potential, k_B is the Boltzmann constant, $v_F = 10^6$ m/s is the Fermi velocity, and $\Gamma = e v_F^2 / 2\mu_c$ is the charged particle scattering rate. The scattering rate for graphene used here is realistic for multilayer structures, as verified by previously reported relevant experiments.⁴⁵ Graphene's optical conductivity is divided into the intraband

and interband parts, which correspond to free carrier absorption and transition from the valence band to the conduction band, respectively. In Eq. (2), the first term is due to intraband contribution and the second term is related to interband transitions contribution. While the closed-form approximations are presented for intraband and interband transitions contribution under the condition of $K_B T \ll |\mu_c|$ and $K_B T \ll \hbar\omega$,⁴⁶ they are not strong assumptions for the high ambient temperature of thermal emitters; thus, the general form in Eq. (2) is

numerically evaluated in our study to obtain a more accurate refractive index of graphene. The dielectric permittivity of monolayer graphene is given by $\epsilon_G(\omega, \mu_c, \Gamma, T) = i\sigma_d/\omega\epsilon_0 t_G$, where t_G is the thickness of a single graphene layer and ϵ_0 is the free-space electric permittivity.

The zero-bandgap and the linear dispersion of graphene imply that there will always be an electron-hole pair with high carrier mobility for broadband illumination, which is very different from semiconductors with bandgap and parabolic dispersion relations. The contributions of intraband and interband transitions in the optical conductivity significantly depend on the carrier density, so that each part has different strength at different frequency ranges. These contributions are also directly related to the chemical potential in graphene. By increasing the chemical potential, the absorption due to the interband transition contribution is reduced by Pauli blocking because the vacant states in the conduction band are all occupied when the pumping light is intense enough for a specific relaxation process.⁴⁷ In other words, graphene acts like a semi-metal with an electrically variable bandgap because the interband transition contribution significantly decreases behaving as a step-like function with a threshold $2|E_F|$ (small value when the photon energy is below the threshold and significant value when the photon energy is above the threshold). This effect leads to an electrically controllable absorption that is proportional to the real part of the optical conductivity.⁴⁸

For short wavelengths (visible and near-IR), graphene's optical conductivity is dominated by interband transitions contribution, making the real and imaginary parts of graphene's refractive index nearly independent of the chemical potential as shown in Figs. 2(a) and 2(b). For longer wavelengths in the mid-infrared range, the intraband transition contribution becomes comparable with the interband transition contribution so that the control over intraband transitions and consequently the refractive index can be obtained by tuning the chemical potential in graphene. While this control is increased in far-infrared and THz ranges, these wavelengths correspond to weak thermal power (low-temperature substrate). Two important properties that are required for the proposed device are strong thermal emission and highly tunable graphene refractive index via the chemical potential. Both of these properties are satisfied at the wavelength of $3.34\ \mu\text{m}$ that we chose for our design. We note that, if we choose a different wavelength of operation at which both of these properties are satisfied, the results and conclusions of this paper will still hold. The maximum emission of a blackbody at the mid-infrared range with the peak at $\lambda = 3.34\ \mu\text{m}$ is considered corresponding to thermal radiation at an ambient temperature of 873 K. For infrared radiation at this temperature, our results from the Kubo formula show the larger contribution of intraband transitions to the total optical conductivity of graphene and thereby even better control over its refractive index. For other materials such as hBN, SiC, and W, the wavelength-dependent indices of refraction (both real and imaginary parts) are obtained from experimental data.^{49,50} All materials used in the structure can tolerate high temperatures due to their high melting points,³⁴ and the effect of layer thickness variations due to thermal expansion

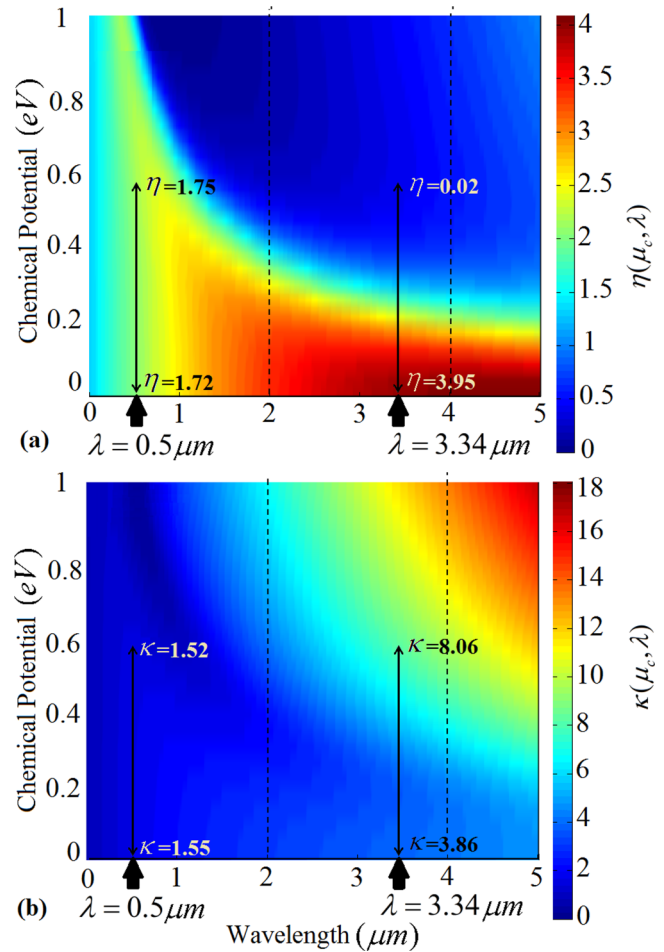


FIG. 2. (a) Real and (b) imaginary parts of the refractive index obtained by the Kubo formalism as well as the equivalent changes in their values for visible and infrared radiation for chemical potential of $\mu_c = 0.0\ \text{eV}$ and $\mu_c = 0.6\ \text{eV}$. The refractive index of graphene is depicted at the ambient temperature of 873 K corresponding to the maximum emission of a blackbody at the mid-infrared range with the peak at $\lambda = 3.34\ \mu\text{m}$. For visible wavelength, the graphene optical conductivity is dominated by interband transitions contribution, making the real and imaginary portions of graphene's refractive index nearly independent of the chemical potential. For mid-infrared wavelengths, the intraband transition becomes comparable with the interband transition contribution; thereby, the control over the intraband transition and consequently the refractive index can be obtained by tuning of the chemical potential in graphene.

on emittance/absorptance can be neglected. Similarly, the possible thickness variations of hBN and SiC layers due to the manufacturing process have a negligible effect on the emittance/absorptance spectra, demonstrating the robustness of the optimized aperiodic multilayer structure. Multilayer graphene-based devices, such as the one proposed in our paper, have been previously reported in the literature. The layers in such devices can be grown by methods such as molecular beam epitaxy (MBE) and plasma-enhanced chemical vapor deposition (PECVD).⁴⁵ Graphene flakes can be deposited by mechanical exfoliation and confirmed to be monolayers with Raman spectroscopy.⁴⁵ The chemical potential of graphene can be adjusted by applying an external voltage. The electrodes required to apply the voltage can be deposited by laser lithography, electron-beam evaporation of the metals, and lift-off fabrication processes.⁴⁵

III. RESULTS AND DISCUSSION

We optimize multiple aperiodic multilayer structures with a different number of graphene layers to determine the best dimensions of thermal emitters for the sake of improved selectivity, tunability, and switchability. Figure 3(a) shows five aperiodic thermal emitters including alternating layers of hBN insulator and graphene (black lines) with 8, 13, 23, 28, and 32 layers of graphene. For a fair comparison, the overall thicknesses of these structures are kept approximately equal, $1\ \mu\text{m}$ to minimize the potential effect of the total thicknesses. Figure 3(b) shows $\bar{\mu}(\lambda)$ [Eq. (2)] as a function of wavelength for the structure. It can be observed that through the interaction of the normal light incidence with the graphene-based nanostructures, all the proposed thermal emitters exhibit almost perfect emission at $\lambda = 3.34\ \mu\text{m}$ and enable narrowband infrared emittance. Even though the structure is optimized to achieve near perfect emittance at a particular wavelength, almost perfect impedance matching is achieved at multiple other wavelengths, which leads to the multiple peaks in the radiated power.⁴² The blackbody bandwidth of $2.7\ \mu\text{m}$ at $T = 873\ \text{K}$ reduces to $0.33\ \mu\text{m}$ for the structure with eight graphene layers, showing more than eight times narrower bandwidth compared to the blackbody radiation. Interestingly, the increase in the number of graphene layers does not result in narrower thermal emission. Thus, the bandwidth of the power emitted from the structure with the smallest amount of graphene layers, i.e., eight, is narrower than the one with the largest number of graphene layers, i.e., 32. However, this increase in the number of graphene layers decreases the strength of undesired power emitted at shorter wavelengths. Figure 4(a) shows the profile of the electric field amplitude normalized with respect to the field amplitude of the incident plane wave at $\lambda = 3.34\ \mu\text{m}$ for varying the chemical potential in the optimized structure with 23 graphene layers. It can be observed for $\mu_c = 0.0\ \text{eV}$, at which the structure is optimized to achieve maximum absorptance, that

the electric field amplitude of normal light incidence is almost flat in air. This property suggests that the reflectance of the structure is almost zero, and the absorptance is therefore almost unity. We found that, as the angle of incidence increases, the peak emittance wavelength shifts toward shorter wavelengths. In addition, increasing the angle of incidence decreases the peak emittance. Figure 4(b) shows the contribution of each graphene layer to the total emittance for $\mu_c = 0.0\ \text{eV}$, $0.4\ \text{eV}$, and $1.0\ \text{eV}$. It is obvious that the contribution of graphene layers to the total power emitted from the proposed structure drastically decreases by increasing the chemical potential. The relative contribution to the energy absorbed in the aperiodic multilayer structures is proportional to the product of the square of the field amplitude, the absorption coefficient, and the real part of graphene's refractive index,⁵¹ which can be manipulated by changing the chemical potential of graphene. The change in the properties of the thermal emittance, induced by changing the chemical potential of the graphene layers, enables an electrically controllable thermal emitter.

Figures 5(b)–5(f) depict the effect of the increase in the chemical potential on the normalized power emitted from the five optimized structures with 8, 13, 23, 28, and 32 layers of graphene, and the thermal power emitted from bulk tungsten at $T = 873\ \text{K}$ is shown in Fig. 5(a) as a reference. The comparison indicates that our graphene-based aperiodic multilayer structures enable not only the narrowband thermal emittance at a mid-infrared wavelength but also provide tunable and switchable thermal emitters. For the optimized thermal emitter with eight graphene layers in Fig. 5(b), it can be observed that the increase in the chemical potential results in a spectral shift toward shorter wavelengths, and in narrower thermal emission. Comparing these results to the ones for the other optimized structures with a more substantial number of graphene layers in Figs. 5(c)–5(f), one can notice the more pronounced effect of chemical potential variation

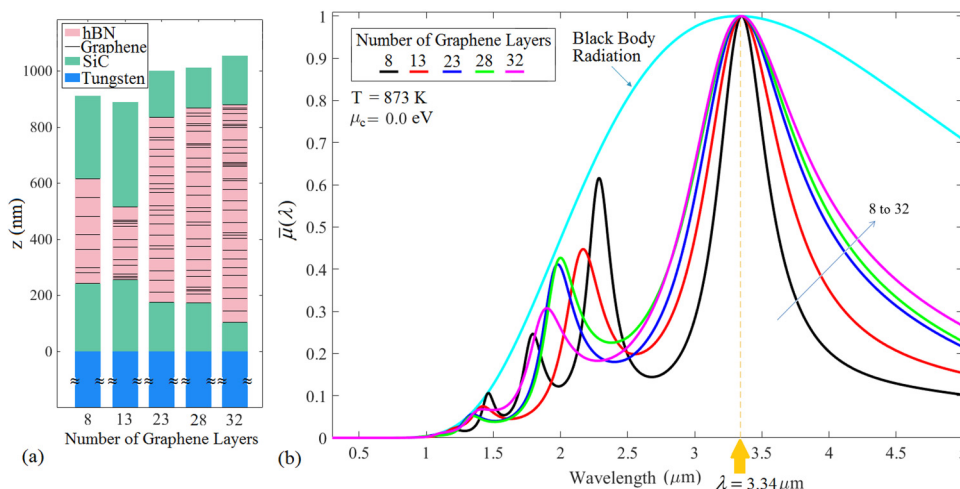


FIG. 3. (a) Five optimized aperiodic multilayer structures with 8, 13, 23, 28, and 32 layers of graphene at $\lambda = 3.34\ \mu\text{m}$, $\mu_c = 0.0\ \text{eV}$, and $T = 873\ \text{K}$. The overall thicknesses of these structures are kept at $\sim 1\ \mu\text{m}$ for a fair comparison, minimizing the potential effect of the total thicknesses. (b) Normalized power radiated per unit area and unit wavelength in the normal direction $\bar{\mu}(\lambda)$ of Fig. 1, as a function of wavelength. The optimized thermal emitters exhibit perfect emittance at $\lambda = 3.34\ \mu\text{m}$, providing narrowband infrared emittance. The increase in the number of graphene layers does not result in narrower thermal emission, but this increases the tunability and the switchability of thermal emittance as shown in Figs. 7 and 8. The thicknesses of each layer are in the supplemental material.

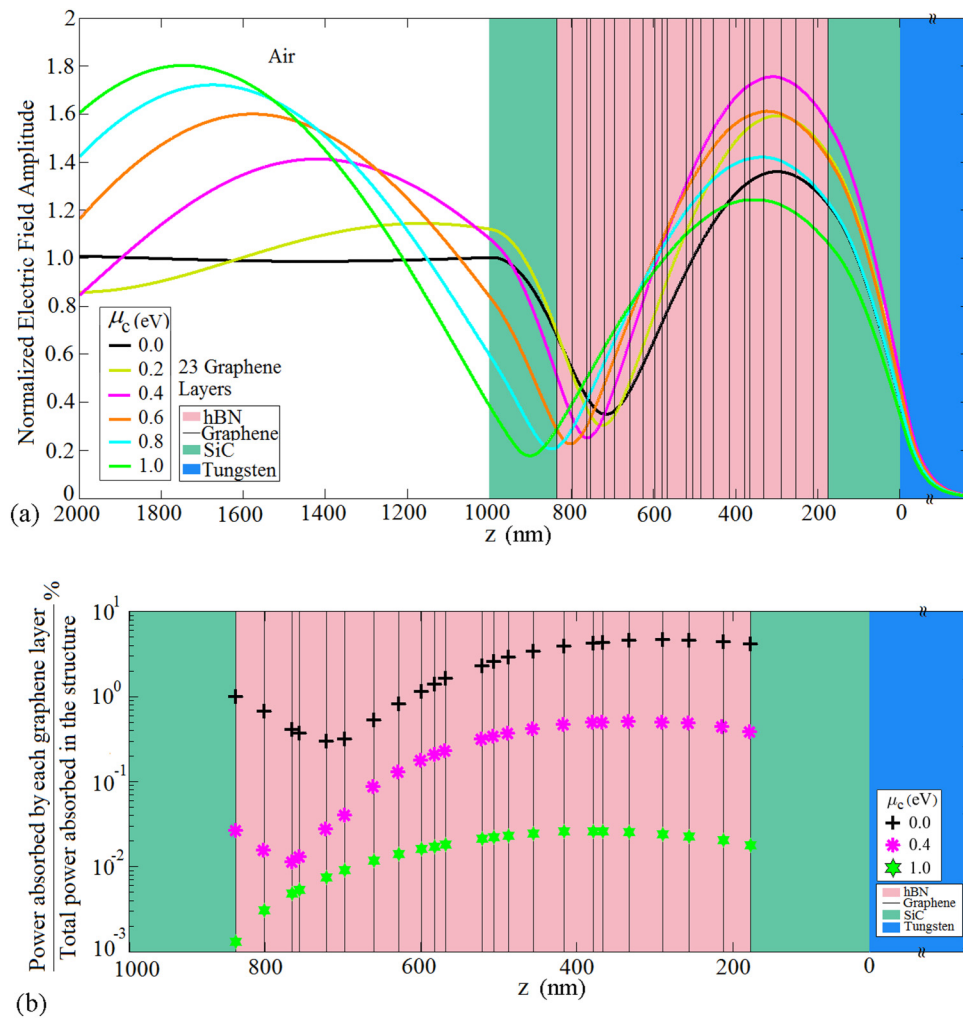


FIG. 4. (a) Profile of electric field amplitude normalized concerning the field amplitude of the incident plane wave for the optimized structure for the parameters given in Fig. 3 with 23 graphene layers at $\lambda = 3.34 \mu\text{m}$. For the chemical potential of $\mu_c = 0.0$ eV, at which the structure is optimized to achieve maximum absorptance, the electric field amplitude is almost flat in air. This effect suggests that the reflectance of the structure is nearly zero, and the absorptance is therefore nearly unity. (b) The percentage of the power absorbed inside each graphene layer to the total power absorbed in the structure shows an order of magnitude reduction by increasing the chemical potential from $\mu_c = 0.0$ eV to 1.0 eV. This is observed due to the change in the real part of graphene's refractive index manipulated by changing the chemical potential of graphene layers.

on the peak emission wavelength and the emission bandwidth as the number of graphene layers is increased.

The switchability can be interpreted from Fig. 5 by looking at the dotted line that corresponds to the wavelength at which the structures are optimized. It can be observed that for the optimized structure with eight graphene layers, changing the chemical potential from 0.0 eV to 1.0 eV does not result in a significant change in the normalized power emitted from the structure. However, the normalized power emitted from the optimized structure with the larger number of graphene layers, i.e., 32, can be almost eliminated by increasing the chemical potential in this range, so that perfect emittance of unity for $\mu_c = 0.0$ eV can be switched to emittance of ~ 0.17 by setting μ_c equal to 1.0 eV. For the rest of the paper, the selectivity, tunability, and switchability of the thermal emittance are studied for the optimized aperiodic multilayer structures with 8, 13, 23, 28, and 32 graphene layers by changing the chemical potential from 0.0 eV to 1.0 eV.

While black-body thermal emission is broadband, narrowband thermal radiation can be achieved using the optimized nanophotonic structures. Figure 6 shows the effect of changing the chemical potential on the bandwidth of the thermal power emitted from the optimized structures with different numbers of graphene layers, i.e., the selectivity of the structure. The bandwidth $\Delta\lambda$ is measured at wavelengths at which the normalized power emitted becomes $0.7 \times \max[\bar{\mu}(\lambda)]$. We observe that for all the optimized structures, the selectivity of thermal radiation in wavelength becomes stronger by increasing the chemical potential. At $\mu_c = 0.0$ eV, the arrangement with eight graphene layers has the power spectrum with the narrowest bandwidth, $\Delta\lambda = 0.315 \mu\text{m}$, i.e., better selectivity, while the power emitted from the structure with 32 graphene layers has about three times broader bandwidth. However, the larger number of graphene layers in the construction provides stronger control of the bandwidth by increasing the chemical potential. The power emitted from the structure with 32 graphene layers becomes three times

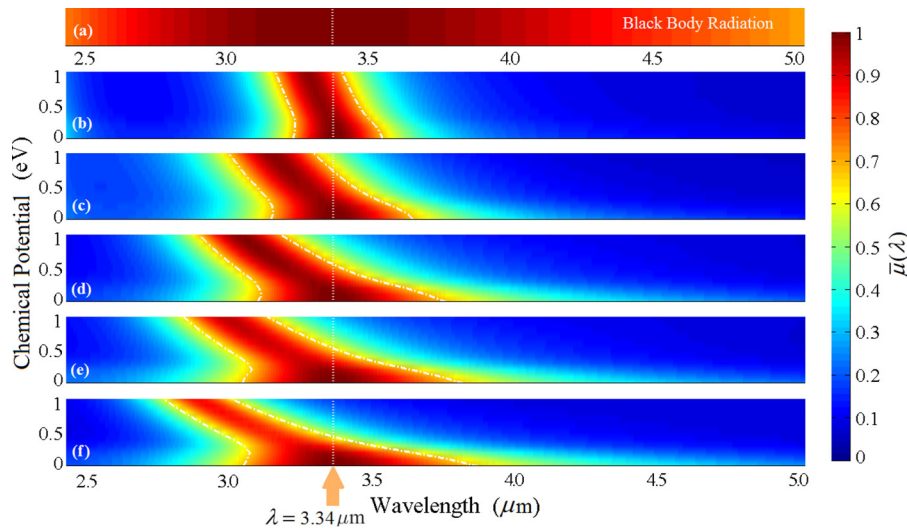


FIG. 5. (a) Normalized thermal power emitted $\bar{\mu}(\lambda)$ per unit area and unit wavelength in the normal direction from bulk tungsten versus wavelength and chemical potential at $T=873$ K for the five optimized structures with (b) 8, (c) 13, (d) 23, (e) 28, and (f) 32 layers of graphene as shown in Fig. 3(a). The optimized graphene-based aperiodic multilayer structures enable narrowband thermal emission in comparison with blackbody thermal radiation in (a). The increase in the chemical potential results in a spectral shift toward shorter wavelength, enabling the electrically tunable thermal emitter, in which the range of tunability increases by increasing the number of graphene layers. The dotted vertical line shows the wavelength of $\lambda = 3.34 \mu\text{m}$ at which the structure is optimized, and the dash-dotted lines correspond to $0.7 \times \max[\bar{\mu}(\lambda)]$, which is used to define the bandwidth of the emission. The thermal emittance from the optimized structure with a larger number of graphene layers can be almost entirely eliminated by increasing the chemical potential so that perfect emittance of unity for the structure with 23 graphene layers can be switched to zero by setting μ_c equal to 1.0 eV.

narrower, changing from $\Delta\lambda = 0.874 \mu\text{m}$ to $0.256 \mu\text{m}$ by increasing the chemical potential from 0.0 eV to 1.0 eV, while the bandwidth of the eight-layer graphene structure only varies from $\Delta\lambda = 0.315 \mu\text{m}$ to $0.234 \mu\text{m}$ for the same change in the chemical potential. As such, the nanophotonic structure with 32 layers of graphene enables stronger selectivity for thermal emission, which is electrically controllable by tuning the chemical potential of graphene layers.

Figure 7 shows the effect of changing the chemical potential on the tunability of the thermal power emitted from the optimized structures with different numbers of graphene layers. We see that the normalized power emitted from all the structures is shifted to lower wavelengths by increasing the chemical potential in graphene. The range of tunability is increased by increasing the number of graphene layers in the aperiodic multilayer structures. For instance, the shift of the

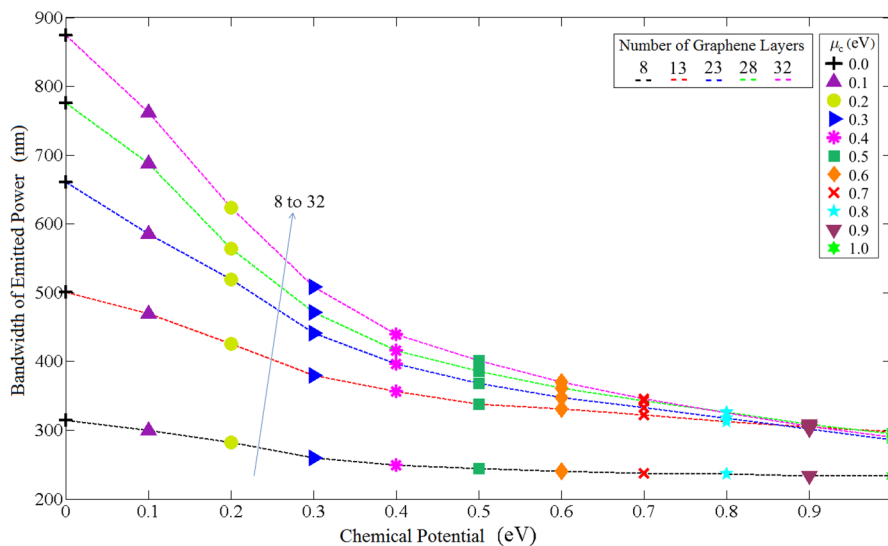


FIG. 6. Bandwidth $\Delta\lambda$, i.e., selectivity, of the thermal power emitted from the optimized structures with different numbers of graphene layers versus chemical potential. The bandwidth is measured at the wavelengths at which the normalized power emitted becomes $0.7 \times \max[\bar{\mu}(\lambda)]$. The thermal emittance becomes more selective due to increasing the chemical potential for all the optimized structures. The structure with eight graphene layers shows the narrower bandwidth for $\mu_c = 0.0$ eV, $\Delta\lambda = 0.315 \mu\text{m}$, but the larger number of graphene layers in the structure provides stronger control over the bandwidth by increasing the chemical potential. By increasing the chemical potential from 0.0 eV to 1.0 eV, the thermal emittance from the structure with 32 graphene layers becomes three times narrower, changing from $\Delta\lambda = 0.874 \mu\text{m}$ to $0.286 \mu\text{m}$, while the bandwidth of the eight layer graphene structure only varies from $\Delta\lambda = 0.315 \mu\text{m}$ to $0.234 \mu\text{m}$. All other parameters are as in Fig. 3(a).

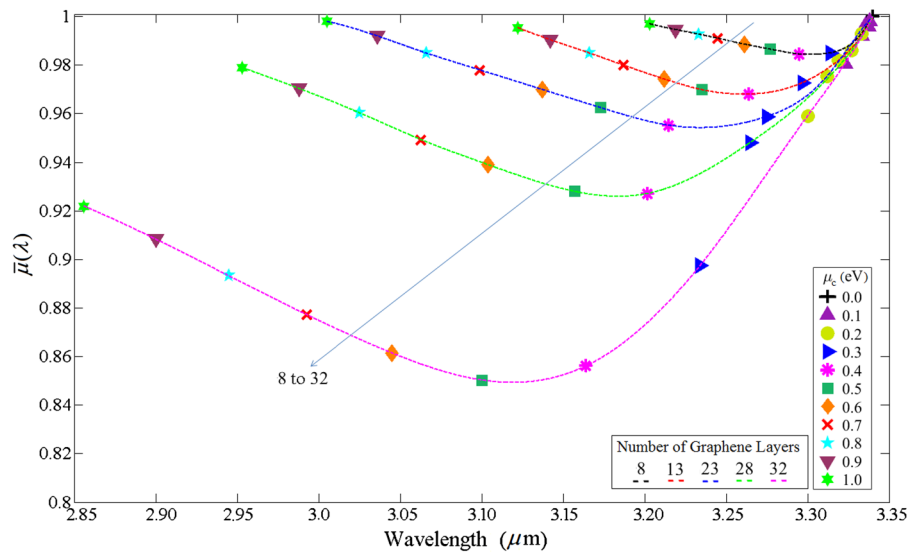


FIG. 7. The tunability of the peak normalized power emitted per unit area and unit wavelength in the normal direction for the optimized structures with a different number of graphene layers when the chemical potential is varied. The range of tunability is increased by increasing the number of graphene layers in the aperiodic multilayer structures as can also be observed from Fig. 5. By increasing μ_c from 0.0 eV to 1.0 eV, the arrangement with 32 graphene layers shows ~ 3.5 times larger shift of the peak emission for the structure with eight graphene layers, changing from $\lambda = 3.34 \mu\text{m}$ to $2.85 \mu\text{m}$. Despite the tunability of the structures, the normalized thermal emittance from the structures deviates from the one for perfect emitters, especially in the middle of the chemical potential range. All other parameters are as in Fig. 3(a).

peak emission for the structure with 32 graphene layers is ~ 3.5 times larger than the one for the structure with eight graphene layers. However, the normalized peak power emitted from the structures deviates from the one for perfect emitters, especially in the middle of the chemical potential range. Overall, the aperiodic multilayer structures enable a tunable thermal emitter that can be electrically controlled by changing the chemical potential in graphene layers.

Figure 8 shows the effect of changing the chemical potential on the thermal power emitted at $\lambda = 3.34 \mu\text{m}$ for the optimized structures with different numbers of graphene layers. We observe that the normalized power emitted for all the optimized structures significantly decreases by increasing the chemical potential in graphene layers. For instance, by

increasing the chemical potential from 0.0 eV to 1.0 eV, the normalized power emitted from the structure with eight graphene layers decreases $\sim 25\%$, changing from the perfect value of unity to ~ 0.75 . The range of change in thermal emission increases by increasing the number of graphene layers in the aperiodic multilayer structures, so that for the structure with 32 graphene layers, the normalized emitted power at $\mu_c = 1.0$ eV decreases by $\sim 83\%$, which is about 4.5 times larger decrease than for the structure with eight graphene layers. As such, the proposed nanophotonic structure can decrease the thermal power emitted from the tungsten substrate, indicating a promising structure to use as switchable thermal power that can be electrically controlled by changing the chemical potential of graphene layers.

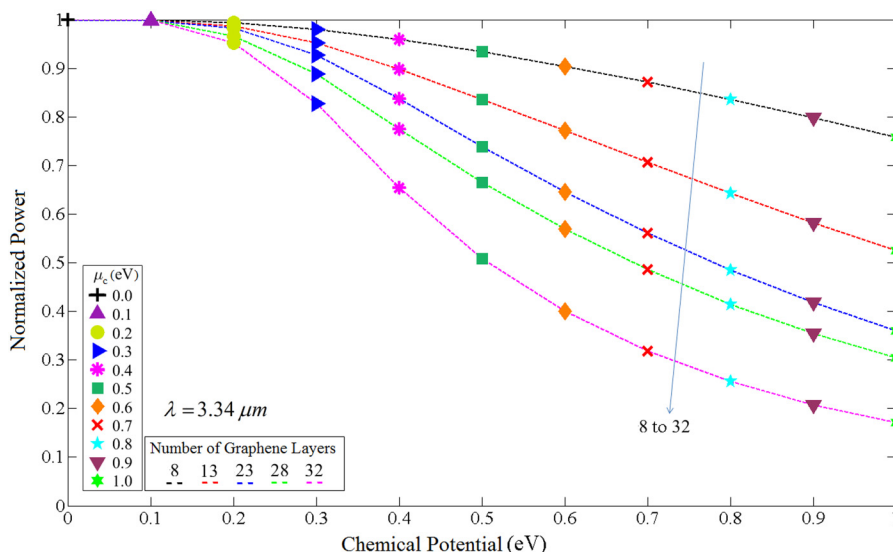


FIG. 8. Switchability of the emitted thermal power from the optimized structures with a different number of graphene layers as the chemical potential is varied at $\lambda = 3.34 \mu\text{m}$. The normalized thermal emittance of all the optimized structures can be significantly decreased at this wavelength by increasing the chemical potential of graphene layers. By increasing the chemical potential from 0.0 eV to 1.0 eV, the normalized thermal emittance from the structures with 8 and 32 graphene layers decrease by $\sim 25\%$ and $\sim 83\%$, respectively, indicating 4.5 times stronger switchability.

IV. CONCLUSION

The spectral characteristics of the radiated thermal power are dictated by the electromagnetic energy density and emissivity, which are ordinarily fixed properties of the material and temperature. In this paper, we presented new graphene-based aperiodic multilayer structures as electrically controllable mid-infrared thermal sources. More specifically, we optimized five aperiodic multilayer structures with 8, 13, 23, 28, and 32 layers of graphene using the genetic optimization algorithm to study the selectivity, tunability, and switchability of thermal emitters by varying the chemical potential of graphene. Despite the broadband spectra of thermal radiation at the infrared range, all the graphene-based thermal emitters enable narrowband emitted power, i.e., more considerable selectivity. We demonstrate that the increase in the number of graphene layers enhances the effect of the chemical potential, resulting in more substantial tunability so that the shift of power emitted from the structure with 32 graphene layers is ~ 3.5 times larger than that of the structure with eight graphene layers. The increase in the number of graphene layers also enhances the switchability by changing the chemical potential so that the thermal power emitted from the structure with 32 graphene layers has ~ 4.5 times stronger decreases than for the structure with eight graphene layers. The dynamic control of the proposed graphene-based aperiodic multilayer structures, electrically by changing the chemical potential of graphene layers, could pave the way to a new class of tunable and switchable thermal sources in the infrared range of the electromagnetic spectrum.

SUPPLEMENTARY MATERIAL

See [supplementary material](#) for the thicknesses of optimized graphene-based aperiodic multilayer structures depicted in Fig. 3(a).

- ¹X. Liu, T. Tyler, T. Starr, A. F. Starr, N. M. Jokerst, and W. J. Padilla, *Phys. Rev. Lett.* **107**, 045901 (2011).
- ²N. Liu, M. Mesch, T. Weiss, M. Hentschel, and H. Giessen, *Nano Lett.* **10**, 2342–2348 (2010).
- ³W. R. Chan, P. Bermel, R. C. Pilawa-Podgurski, C. H. Marton, K. F. Jensen, J. J. Senkevich, J. D. Joannopoulos, M. Soljačić, and I. Celanovic, *Proc. Natl. Acad. Sci. U.S.A.* **110**, 5309–5314 (2013).
- ⁴H. Wang and L. Wang, *Opt. Express* **21**, A1078–A1093 (2013).
- ⁵H. Miyazaki, T. Kasaya, M. Iwanaga, B. Choi, Y. Sugimoto, and K. Sakoda, *Appl. Phys. Lett.* **105**, 121107 (2014).
- ⁶G. Bruccoli, P. Bouchon, R. Haïdar, M. Besbes, H. Benisty, and J.-J. Greffet, *Appl. Phys. Lett.* **104**, 081101 (2014).
- ⁷B. Liu, Y. Liu, and S. Shen, *Phys. Rev. B* **90**, 195411 (2014).
- ⁸J. A. Schuller, T. Taubner, and M. L. Brongersma, *Nat. Photonics* **3**, 658–661 (2009).
- ⁹E. Rephaeli, A. Raman, and S. Fan, *Nano Lett.* **13**, 1457–1461 (2013).
- ¹⁰J.-J. Greffet, R. Carminati, K. Joulain, J.-P. Mulet, S. Mainguy, and Y. Chen, *Nature* **416**, 61–64 (2002).
- ¹¹H. Sai, Y. Kanamori, and H. Yugami, *Appl. Phys. Lett.* **82**, 1685–1687 (2003).
- ¹²C. M. Cornelius and J. P. Dowling, *Phys. Rev. A* **59**, 4736 (1999).
- ¹³S.-Y. Lin, J. Moreno, and J. Fleming, *Appl. Phys. Lett.* **83**, 380–382 (2003).

- ¹⁴S. Maruyama, T. Kashiwa, H. Yugami, and M. Esashi, *Appl. Phys. Lett.* **79**, 1393–1395 (2001).
- ¹⁵F. Kusunoki, J. Takahara, and I. Kobayashi, *Electron. Lett.* **39**, 23–24 (2003).
- ¹⁶G. Biener, N. Dahan, A. Niv, V. Kleiner, and E. Hasman, *Appl. Phys. Lett.* **92**, 081913 (2008).
- ¹⁷S. Thongrattanasiri, F. H. Koppens, and F. J. G. De Abajo, *Phys. Rev. Lett.* **108**, 047401 (2012).
- ¹⁸M. Laroche, R. Carminati, and J.-J. Greffet, *Phys. Rev. Lett.* **96**, 123903 (2006).
- ¹⁹D. Smith, S. Schultz, N. Kroll, M. Sigalas, K. Ho, and C. Soukoulis, *Appl. Phys. Lett.* **65**, 645–647 (1994).
- ²⁰E. Brown and O. McMahon, *Appl. Phys. Lett.* **67**, 2138–2144 (1995).
- ²¹D. L. Chan, M. Soljačić, and J. Joannopoulos, *Opt. Express* **14**, 8785–8796 (2006).
- ²²I. Celanovic, N. Jovanovic, and J. Kassakian, *Appl. Phys. Lett.* **92**, 193101 (2008).
- ²³F. Reif, *Fundamentals of Statistical and Thermal Physics* (Waveland Press, 2009).
- ²⁴I. Puscasu and W. L. Schaich, *Appl. Phys. Lett.* **92**, 233102 (2008).
- ²⁵L. Wang, B. Lee, X. Wang, and Z. Zhang, *Int. J. Heat Mass Transf.* **52**, 3024–3031 (2009).
- ²⁶H. Miyazaki, K. Ikeda, T. Kasaya, K. Yamamoto, Y. Inoue, K. Fujimura, T. Kanakugi, M. Okada, K. Hatade, and S. Kitagawa, *Appl. Phys. Lett.* **92**, 141114 (2008).
- ²⁷B. Liu, W. Gong, B. Yu, P. Li, and S. Shen, *Nano Lett.* **17**, 666–672 (2017).
- ²⁸B. Liu, J. Li, and S. Shen, *ACS Photonics* **4**, 1552–1557 (2017).
- ²⁹J. Mason, S. Smith, and D. Wasserman, *Appl. Phys. Lett.* **98**, 241105 (2011).
- ³⁰C. Wu, B. Neuner III, J. John, A. Milder, B. Zollars, S. Savoy, and G. Shvets, *J. Opt.* **14**, 024005 (2012).
- ³¹W. Streyer, S. Law, A. Rosenberg, C. Roberts, V. Podolskiy, A. Hoffman, and D. Wasserman, *Appl. Phys. Lett.* **104**, 131105 (2014).
- ³²T. Inoue, M. De Zoysa, T. Asano, and S. Noda, *Optica* **2**, 27–35 (2015).
- ³³J. Cong, B. Yun, and Y. Cui, *Opt. Express* **21**, 20363–20375 (2013).
- ³⁴K. S. Novoselov, V. Fal, L. Colombo, P. Gellert, M. Schwab, and K. Kim, *Nature* **490**, 192–200 (2012).
- ³⁵P.-Y. Chen and A. Alù, *ACS Nano* **5**, 5855 (2011).
- ³⁶R. Alaei, M. Farhat, C. Rockstuhl, and F. Lederer, *Opt. Express* **20**, 28017–28024 (2012).
- ³⁷H. Wang, Y. Yang, and L. Wang, *J. Opt.* **17**, 045104 (2015).
- ³⁸Z. Fang, Y. Wang, A. E. Schlather, Z. Liu, P. M. Ajayan, F. J. García de Abajo, P. Nordlander, X. Zhu, and N. J. Halas, *Nano Lett.* **14**, 299–304 (2013).
- ³⁹Z. Ni, H. Wang, J. Kasim, H. Fan, T. Yu, Y. Wu, Y. Feng, and Z. Shen, *Nano Lett.* **7**, 2758 (2007).
- ⁴⁰D. Golla, K. Chattrakun, K. Watanabe, T. Taniguchi, B. J. LeRoy, and A. Sandhu, *Appl. Phys. Lett.* **102**, 161906 (2013).
- ⁴¹Y. Jia, H. Zhao, Q. Guo, X. Wang, H. Wang, and F. Xia, *ACS Photonics* **2**, 907 (2015).
- ⁴²C. H. Granier, F. O. Afzal, S. G. Lorenzo, M. Reyes, Jr., J. P. Dowling, and G. Veronis, *J. Appl. Phys.* **116**, 243101 (2014).
- ⁴³T. Stauber, N. Peres, and A. Geim, *Phys. Rev. B* **78**, 085432 (2008).
- ⁴⁴L. Falkovsky and S. Pershoguba, *Phys. Rev. B* **76**, 153410 (2007).
- ⁴⁵M. Furchi, A. Urich, A. Pospischil, G. Lilley, K. Unterrainer, H. Detz, P. Klang, A. M. Andrews, W. Schrenk, and G. Strasser, *Nano Lett.* **12**, 2773 (2012).
- ⁴⁶G. W. Hanson, *J. Appl. Phys.* **103**, 064302 (2008).
- ⁴⁷Z. Sun, T. Hasan, F. Torrisi, D. Popa, G. Privitera, F. Wang, F. Bonaccorso, D. M. Basko, and A. C. Ferrari, *ACS Nano* **4**, 803–810 (2010).
- ⁴⁸T. Stauber, D. Noriega-Pérez, and J. Schliemann, *Phys. Rev. B* **91**, 115407 (2015).
- ⁴⁹L. Aksyutov, *J. Appl. Spectrosc.* **26**, 656–660 (1977).
- ⁵⁰S. Singh, J. Potopowicz, L. Van Uitert, and S. Wemple, *Appl. Phys. Lett.* **19**, 53–56 (1971).
- ⁵¹L. A. Pettersson, L. S. Roman, and O. Inganäs, *J. Appl. Phys.* **86**, 487–496 (1999).